BMC Veterinary Research

RESEARCH

Open Access

Tumor immune microenvironment and immune phenotypes in PD-L1-tested canine urothelial carcinoma

L.V. Muscatello[1], G. D'Annunzio[2*], T. Franceschini[3], C. Tugnoli[1], A. Grillini[1], B. Bacci[1], G. Avallone[1], P. Valenti[4], A. Giuliano[5], M. Fiorentino[1], D. Volpatti[6] and G. Sarli[1]

Abstract

Immune checkpoint inhibition (ICI) is a promising therapeutic strategy for counteracting tumor immune evasion. The therapeutic response largely depends on interactions between cancer cells and the tumor immune microenvironment (TIME). This study aimed to characterize the TIME and its relationship with the immune checkpoint ligand Programmed Death-Ligand 1 (PD-L1) in canine urothelial carcinomas (UCs). UCs were retrospectively selected and tested for PD-L1 using single-antibody immunohistochemistry. Multiplex immunohistochemistry was performed using anti-CD3, -CD20, and -IBA1 antibodies, to co-localize the immune cells (ICs). Both ICs and PD-L1 expression were quantified with computer-assisted image analysis (QuPath software). Based on the spatial distribution and density of ICs, tumors were classified in three distinct immune phenotypes: immune-inflamed, immune-excluded, and immune-desert. Among the 49 UCs analyzed, 11 (22%) were PD-L1+. Forty carcinomas were classified as immune-inflamed (9 PD-L1+; 31 PD-L1-), 7 as immune-excluded (2 PD-L1+; 5 PD-L1-), and 2 as immune-desert (PD-L1-). Macrophages and T-cells were the most numerous ICs, while B-cells were significantly fewer ($p < 0.0001$). PDL1 + tumors exhibited a significantly higher number of macrophages compared to PD-L1- tumors ($p = 0.003$). Immuno-inflamed tumors showed a higher density of T cells ($p = 0.01$) and a lower macrophages-to-T lymphocytes ratio ($p = 0.02$) compared to immune-excluded and immune-desert phenotypes. In summary, most UCs were immune-inflamed and T-cell rich; a subset of tumors was PDL1 + and associated with a higher number of macrophages. Further characterization of T lymphocytes and macrophages polarization is necessary to better stratify the immune response.

Keywords Multiplex immunohistochemistry, Computer-aided image analysis, Canine urothelial carcinoma, PD-L1, Tumor immune microenvironment, Immune-inflamed, Immune-excluded, Immune-desert

*Correspondence:
G. D'Annunzio
giulia.dannunzio@izsler.it
[1]University of Bologna, Bologna, Italy
[2]Experimental Zooprophylactic Institute of Lombardia and Emilia-Romagna "Bruno Ubertini", Brescia, Italy
[3]Pathology Unit, DIAP-Dipartimento Interaziendale di Anatomia Patologica di Bologna, Maggiore Hospital-AUSL Bologna, Bologna, Italy
[4]Clinica Veterinaria Malpensa AniCura, Samarate, Samarate, Varese, Italy
[5]Harvest Veterinary Oncology Center Kwai Fong, Hong Kong, Kowloon, China
[6]University of Udine, Udine, Italy

Introduction

Although infrequent, urothelial carcinoma (UC), is the most common neoplasm of the urinary bladder in dogs [5]. Median survival time in treated patients varies based on the studies and ranges between 6 and 12 months or more [5]. Due to its invasive feature, canine UC is considered a spontaneous model for human muscle-invasive urothelial carcinoma [5]. In humans, immune checkpoint inhibitory therapy is the most recent frontier in counteracting tumor immune evasion by targeting and blocking the PD-1/PD-L1 axis. Two phase three trials with the immune checkpoint inhibitors (ICI) anti PD-1 Nivolumab [2] and anti PD-L1 Atezolizumab [14] demonstrated that immunotherapy was superior to placebo or platinum-based chemotherapy in the neoadjuvant and metastatic setting of human urothelial carcinoma. Although positive results have been obtained, it has been demonstrated that the response to ICI is strictly dependent on the interaction between cancer cells and Tumor Immune Micro-Environment (TIME), such as the abundance and activation of CD8 + T cells, the presence of other immune cells and local cytokine signaling, resulting in a plastic interaction [31]. Therefore, the TIME characterization becomes essential to predict the response to immunotherapy.

Based on the immunophenotypic and spatial composition of the TIME, neoplasm can be classified as immunologically active or "hot", namely immune-inflamed phenotype, characterized by tumor-infiltrating lymphocytes within the tumor bed [31]. Conversely, tumor can be categorized as immunologically inactive or "cold", so called immune-desert phenotype, when immune cells are absent both outside and within the tumor. A special type is the immune-excluded phenotype, in which the tumor is immune cell-rich, but the T lymphocytes fail to infiltrate the tumor and are located at the invasion front or within the tumor stroma. It is not clear whether the lack of infiltration into the tumor results from insufficient stimulation or whether infiltration is physically prevented by other pro-tumorigenic factors, such as the presence of macrophages at the invasion front [31].

PD-L1 is a recent topic of investigation in canine tumors [18–21, 28]. A previous study focused on standardizing the immunohistochemical assessment of canine tissues [21], and considered only tumors with membranous expression to be positive, in alignment with human studies [1]. The same study reported that PD-L1 labeled 11% of canine UC [21]. Building upon these findings, in the present work we aimed to:

1) characterize the TIME in canine UC using multiplex immunohistochemistry, classifying tumors into distinct immunological phenotypes based on the spatial distribution of immune cell subsets.
2) investigate the associations between the TIME profiles, immunological phenotypes, and PD-L1 expression.

Material and methods

Case selection

Canine UCs were retrospectively selected from the database of multiple departments: the Pathology Service of the Department of Veterinary Medical Science, University of Bologna, the Department of Veterinary Clinical Science, City University of Hong Kong and the Veterinary Pathology Unit of the Department of Agricultural, Food, Environmental, and Animal Sciences, University of Udine. Samples were available as formalin-fixed paraffin-embedded tissues (FFPE). Hematoxylin and eosin sections were reviewed by two veterinary pathologists, one board certified (L.V.M.) and one experienced pathologist (G.S.), to confirm the diagnosis.

Single antibody immunohistochemistry

Immunohistochemistry with antibody against PD-L1 (PD-L1/CD274 Rabbit pAb, ABClonal, catalog no. A1645) was performed manually according to previous published method [21]. Three-µm-thick sections were dewaxed in xylene substitute solvent and rehydrated. Endogenous peroxidase was blocked by immersion in 3% H_2O_2 diluted in methanol for 30 min. Antigen retrieval was performed using a pH-6.0 citrate buffer (Sigma-Aldrich, Merck KGaA, Darmstadt, Germany) heated for 10 min in a microwave oven at 750 W. Slides were then incubated, for 10 min, in a commercial blocking solution (Super Block, Scytek Laboratories, Logan, Utah, USA). Sections were incubated overnight at 4 °C with antibody against PD-L1 (PD- L1/CD274 Rabbit pAb, ABClonal, catalog no. A1645, dilution 1:400). Antibody binding was visualized using an anti-Polyvalent HRP Polymer (Scytek Laboratories, Logan, Utah, USA). The chromogen DAB (3,3′-diaminobenzidine 0.05% w/v, catalog no. ACB999, Histo-Line Laboratories, Pantigliate, MI, Italy) was used to visualize the reaction. Slides were counterstained with Harris's hematoxylin. Normal canine tonsil and placenta were used as positive controls. For negative controls, the primary antibody was replaced with an irrelevant, isotype- matched antibody, to control for the nonspecific binding of the secondary antibody.

Multiplex immunohistochemistry

The entire staining procedure was performed in an automated immunostainer (Discovery Ultra Roche Diagnostics) on 4 µm thick paraffin-embedded tissue sections. Deparaffinization was done with EZ prep solution and antigen retrieval was done with CC1 solution (Discovery CC1, REF 950 – 500, Ventana Medical Systems, Inc., Arizona, US) at 95°C for 40 min. A triple staining protocol

was used to identify T lymphocytes, B lymphocytes, and macrophages.

CD3 (Roche; rabbit monoclonal Clone 2GV6, ready to use), CD20 (Invitrogen; polyclonal rabbit) at 1:300 dilution and a polyclonal antibody against IBA1 (Novus; goat polyclonal) at 1:2500 dilutions were used as primary antibodies. CD3 was dispensed and incubated for 32 min at 36°C, the slides were treated with rabbit multimer (Rb-HRP, Roche) and subsequently with DISCOVERY ChromoMap DAB Kit for detection of the reaction. IBA1 was dispensed, incubated for 24 min at 36°C and amplified (Amp A e B, Roche). After the sections were treated with mouse multimer (Rb-HRP), finally the slides were processed with the Discovery Purple HRP kit. For the detection of CD20 we proceeded with "option diluent" that blocks nonspecific sites. The antibody was dispensed, incubated for 36 min at 36°C and amplified (Amp A e B). Rabbit multimer (Rb-HRP) served as secondary antibody, followed by the Discovery Teal HRP staining kit. The slides were cleaned by washing with Reaction Buffer.

DISCOVERY ChromoMap DAB Kit (RUO) consist of three different dispensers. "DISCOVERY DAB CM" contains a phosphate buffer, diaminobenzidine (DAB), and gentamicin sulfate. "DISCOVERY H_2O_2 CM" contains a phosphate buffer and hydrogen peroxide (H_2O_2). "DISCOVERY Copper CM" contains an acetate buffer and cupric sulfate and gentamicin sulfate.

DISCOVERY Purple Kit (RUO) is made of two different dispensers. "DISCOVERY Purple" contains a Purple Chromogen and "DISCOVERY H_2O_2" contains Hydrogen Peroxide in an aqueous solution.

DISCOVERY Teal HRP Kit (RUO) consist of three dispensers. "DISCOVERY Teal HRP H_2O_2" contains a borate buffer and hydrogen peroxide. "DISCOVERY Teal HRP Substrate" contains a borate buffer and a reactant to a component in the Teal Activator. "DISCOVERY Teal HRP Activator" contains a borate buffer and a reactant to a component in the Teal Substrate.

In this staining procedure was also used "Amplification Kit" that utilizes rabbit anti-mouse IgG heavy and light chains, and mouse anti-rabbit IgG heavy chains to bind to the primary antibody, increasing the number of antibodies bound at the site of antigen and increasing the staining intensity.

Rb-HRP (Anti rabbit HRP) is a biotin-free detection systems based on proprietary multimer technology. They consist of a robust chemistry that provides clean background in combination with enhanced specificity and sensitivity, which increases the signal-to-noise ratio.

Computer-aided image analysis

Immunohistochemical glass slides were digitalized using Grundium Ocus 20 (Tampere, Finland) to obtain a whole-slide image (WSI). Computer-aided image analysis was performed using the open-access and open-source software QuPath for digital pathology [3].

First, the tumor area was selected, including tumor cells, intratumoral and peritumoral stroma, and excluding the adjacent normal tissue.

Quantification of immune cells in multiplex immunohistochemistry sections was achieved through the combined detection of object and pixel classification tools. The classifiers, for both using the Random Trees algorithm, were trained to recognized tumor tissue and CD3, CD20 and IBA1 labelled cells. The training was achieved through annotations (average of 20 annotations per variable type) performed under the combined supervision of a board-certified veterinary pathologists (L.V.M.) and a biotechnologist with experience in using QuPath (C.T.).

T lymphocytes, B cells and macrophages were quantified as number of cells in the selected tumor area. To account for differences in tissue area due to variable biopsy sizes, absolute cell counts were normalized to tissue area and reported as the number of cells per median area size (31,931,886.98 μm^2).

PD-L1 expression, macrophage-T lymphocytes ratio and immunological classification

PD-L1 expression was assessed in both tumor cells and tumor-infiltrating immune cells according to a previously published method [21]. PD-L1 scoring was calculated using the Combined Positive Score (CPS), defined as the ratio of the total number of PD-L1–positive cells (including both neoplastic cells and tumor-infiltrating immune cells) to the total number of neoplastic cells, expressed as a percentage. A CPS value ≥ 1% was considered positive.

Manual scoring of PD-L1 was independently performed by three veterinary pathologists, either board-certified or with specific expertise in the field (L.V.M., G.S., G.A.). Representative tumor areas showing PD-L1 expression and immune cell infiltration were selected for analysis. Images from these areas were acquired and processed using ImageJ for manual counting, which was performed on a minimum of 500 tumor cells per case, including all PD-L1–positive immune cells within the selected fields. CPS values were subsequently calculated based on the results of this manual count.

PD-L1-positive macrophages were counted manually, to discriminate morphology among the immune cells, across the entire slide. The data was normalized by performing the ratio with the biopsy area (per 1 mm^2).

The macrophage-to-T lymphocyte ratio was obtained with the number of IBA1 + cells divided by the number of CD3 + cells.

The immunophenotypic and spatial composition of the TIME will lead to classify the tumors into distinct immune phenotypes [31]; Binnewies et al., [4]:

- immune-inflamed phenotype: defined by a dense infiltration of immune cells within the tumor parenchyma.
- immune-excluded phenotype: defined by the accumulation of lymphocytes at the invasive margin or in the peritumoral stroma, with scarce or no infiltration into the tumor core; the occasional presence of macrophages within the tumor nests was not considered exclusionary.
- immune-desert phenotype: characterized by a complete absence of lymphocytes both intratumorally and peritumorally; the occasional presence of macrophages within the tumor nests was not considered exclusionary.

The classification of tumor immune phenotypes was based on the qualitative immunohistochemical assessment of the spatial distribution of immune cells. To minimize subjective bias, all cases were independently evaluated in a blinded manner by two observers (L.V.M. and G.S.). Discrepancies were resolved through consensus discussion.

Clinical follow up

Patients were treated with different chemotherapy agents and assessment of response and rechecks performed every 3–6 weeks at clinician discretion, based on RECIST criteria [22]. Tumor-specific survival (TSS) was defined as the time elapsed from the tumor diagnosis to the tumor related death.

Statistics

Statistical analysis was performed with the software GraphPad Prism (version 10.0, La Jolla, San Diego, CA, USA). The normality distribution of the data was assessed with the D'Agostino and Pearson Omnibus test. Data were analyzed with Spearman r, Fisher's exact test, Mann-Whitney test, Kruskal Wallis with Dunn's multiple comparisons tests. To assess inter-observer reliability, the Intraclass Correlation Coefficient (ICC) was calculated [10]. ICC values were interpreted as follows: <0.5 = poor reliability; 0.5–0.75 = moderate reliability; 0.75–0.9 = good reliability; >0.9 = excellent reliability. A p value ≤ 0.05 was considered significant.

Results

Caseload

Forty-nine cases of canine urothelial carcinoma were collected. Of the 49 UCs collected, 11 UCs (22%) were PD-L1+ (Supplemental Fig. 1a). PD-L1 specific labeling was membranous and detected in tumor cells and immune cells (macrophages, lymphocytes and plasma cells). The intraclass correlation coefficient (ICC) for CPS assessment among the three pathologists was 0.82 (95% confident interval = 0.60 to 0.94), indicating good inter-rater reliability. The mean CPS values assessed by each pathologist were as follows:

$$\text{Pathologist 1}: \ 30.73\% \ (\text{SD} = 17.46\%).$$

$$\text{Pathologist 2}: \ 28.00\% \ (\text{SD} = 17.40\%).$$

$$\text{Pathologist 3}: \ 32.91\% \ (\text{SD} = 24.58\%).$$

Immune cells density and topography

Based on the topography of ICs, 40 carcinomas were immune-inflamed (82%; Fig. 1a), 7 were immune-excluded (14%; Fig. 1b), and 2 immune-deserted (4%; Fig. 1c).

Overall, the most numerous ICs were macrophages and T-cells, that were respectively significantly higher than B-cells ($p < 0.0001$ Kruskal Wallis Dunn's multiple comparisons test; Fig. 2a; Supplemental Fig. 1b).

The macrophages to T-lymphocytes ratio was significantly lower in immune-inflamed (mean 1.84% SD = 2.62) compared to immune-excluded and immune-desert phenotypes (mean 7.5% SD = 8.72, $p = 0.02$ Mann-Whitney test; Fig. 2b). T cells number was significantly higher in the immune-inflamed phenotype compared to the other immune phenotypes, immune-excluded and immune-desert ($p = 0.01$ Mann-Whitney test; Fig. 2c). Furthermore, there were no significant differences in the number of B-cells (immune-inflamed vs. other immune phenotypes; $p = 0.20$ Mann-Whitney test) and macrophages in the different immunophenotypes (immune-inflamed vs. other immune phenotypes; $p = 0.80$ Mann-Whitney test). Among the immune-inflamed 9 carcinomas were PD-L1+ (22%) and 31 PD-L1- (78%); two immune-excluded carcinomas were PD-L1+ (28%) and 5 were PD-L1- (71%); both tumors with immune-desert phenotype were PD-L1-. No statistical association was found between PD-L1 expression and immune phenotypes ($p = 0.79$ Fisher's exact test). Macrophages density was higher in PD-L1 + tumors than PD-L1- tumors ($p = 0.003$ Mann-Whitney test; Fig. 2d), supported by a moderate positive correlation between PD-L1 and IBA1 + cells ($p = 0.003$ $R = 0.41$ Spearman test). No statistical correlation between PD-L1 and T and B cells was detected (CD3 and PD-L1 $p = 0.28$ $R = 0.15$; CD20 and PD-L1 $p = 0.23$ $R = 0.17$ Spearman r test).

Because macrophages were the most numerous IC cell population assessed in UCs and PD-L1 + tumors, we tested the possibility of a higher amounts of PD-L1 + macrophages in immune-inflamed vs. immune-excluded PD-L1 + tumor cases. The median number of PD-L1 + macrophages was 1.6/mm² (range 0.6–24.2). No

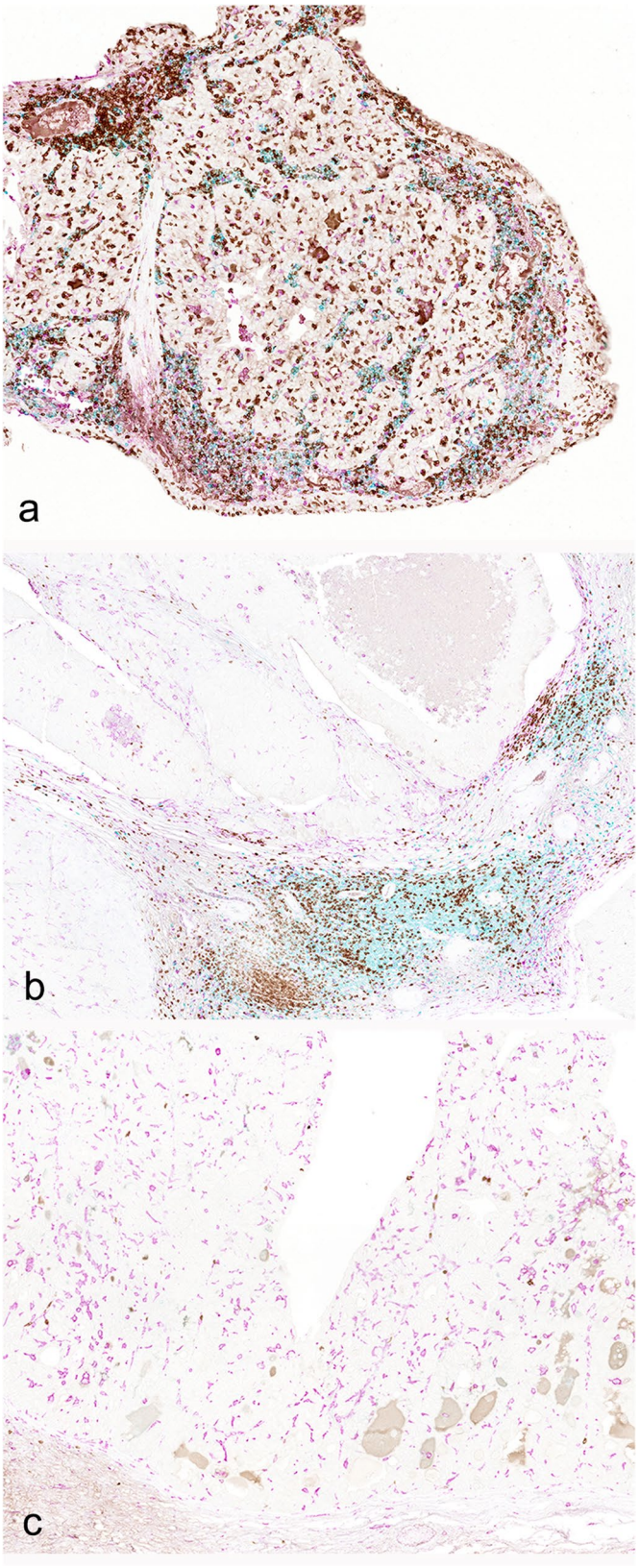

Fig. 1 (See legend on next page.)

(See figure on previous page.)

Fig. 1 Immune phenotype characterized by multiplex immunohistochemistry anti-IBA1 (pink), -CD3 (brown), -CD20 (light blue), canine urothelial carcinoma; **(a)** immune-inflamed phenotype: numerous inflammatory cells infiltrate the tumor bed and are composed of a high number of T lymphocytes and a smaller number of macrophages and B lymphocytes. **b** immune-excluded phenotype: numerous T and B lymphocytes are located at the periphery of the neoplasm and do not infiltrate the tumor bed; only rare macrophages are present inside the tumor. **c** immune-desert phenotype: T and B lymphocytes are totally absent and only rare macrophages are present in the tumor bed

association was observed between the different immunophenotypes ($p = 0.90$, Mann–Whitney test).

Clinical follow up

Median follow up was 238.5 days and follow-up data were available in 12 patients: 9 dogs died from progressive disease and 2 from non-tumor related conditions (1 case due to gastric dilation and volvulus and 1 case due to uroperitoneum developed 1 day after surgery); one case was lost to follow up. Among the deceased patients, 9 UCs had an immune-inflamed phenotype, 2 were immune-excluded and 1 was immune-desert. PD-L1 expression was observed in 2 out of 12 deceased patients (1 immune-inflamed and 1 immune-excluded). The mean TSS of UCs was 295 days (SD = 271.5). The case with the shortest survival was PD-L1 positive and immune excluded (102 days of TSS). No significant differences in TSS were observed between dogs bearing PD-L1 + UCs and those with PD-L1- UCs, even if PD-L1 + UCs had a lower median survival (172 days) than the other group (295 days; $p = 0.16$ Log-rank Mantel-Cox test). Clinical data are summarized in Supplementary Table 1.

Discussion

Immune checkpoint inhibitors (ICIs) are FDA-approved standard of care in several human solid tumors [30]. Markers able to predict the response to ICIs include PD-L1 expression, microsatellites instability and tumor mutational burden [27]. PD-L1 is the most used predictive marker of response to ICIs but there are several limitations related to the pre-analytical and analytical methods; these include but are not limited to formalin fixation, antibody clones, cut-offs selected, and the cell type considered for the evaluation (tumor cells and immune cells) [8]. Additionally, the predictive heterogeneity of PD-L1 is also intrinsic to its biological variability, orchestrated by different TIME components [8]. Resistance mechanisms, including prevention of T cell activity through insufficient immunogenicity, irreversible T cell exhaustion, IFNγ resistance, and the establishment of an immunosuppressive TIME, may affects the ICI response [16].

Considering the plethora of mechanisms involved in tumor immunological response, the study of the immune microenvironment is necessary for a comprehensive approach to its modulation and plasticity.

By analyzing the TIME in the canine UCs, we found that the most represented cells were macrophages, closely followed by T lymphocytes, while B cells were significantly lower. Indeed, tumor associated macrophages (TAMs) are the largest innate immune population of the tumor immune microenvironment and are functionally divided into populations that may have an anti-tumorigenic and a pro-tumorigenic role [31]. Anti-tumorigenic TAMs (M1 polarized), maintain antigen presenting cells function, express high level of MHCII, and have phagocytic and tumor-killing proprieties. Furthermore, they support and activate the adaptive immune response [31]. By contrast, pro-tumorigenic TAMs (M2 polarized) are immunosuppressive, express low level of MHCII and high level of inhibitory molecules, such as PD-1 and PD-L1 [31].

The number of macrophages is significantly increased in human bladder tumor tissue, with M2-polarized macrophages being associated with disease severity and poor prognosis [29, 33]. In our study, IBA1$^+$ cells were not only the most abundant cell population within the tumor microenvironment but also predominated in PD-L1–positive tumors. A similar trend has been observed in human cancers such as nasopharyngeal adenocarcinoma, and gastric, esophageal, and lung carcinomas [9, 15, 24, 34]. The role of tumor-associated macrophages (TAMs) in regulating PD-L1 expression is currently under investigation in human oncology, with several inflammatory cytokine–mediated pathways implicated [35]. Lim et al. reported that TNF-α secreted by TAMs activates the NF-κB pathway, leading to the transactivation of CSN5, which in turn mediates the deubiquitination and stabilization of PD-L1 [17].

The results of our investigation, according to the literature [31], confirmed PD-L1 expressed also by macrophages, suggestive of a pro-tumorigenic activity, but future studies incorporating established M1/M2 markers are essential to conclusively characterize macrophage polarization in canine urothelial carcinoma.

We quantified PD-L1$^+$ macrophage densities in the subset of PD-L1-positive tumors; however, our findings did not show a substantial association with specific immune-inflamed or immune-excluded phenotypes. The small number of PD-L1-positive cases likely limited statistical power and may have impacted these results.

T-lymphocytes are the most important cells of the adaptative anti-tumoral immune response [13, 32]. Different studies have demonstrated that the greater the tumor infiltration of CD8 + T lymphocytes, the better the survival [12, 26] and the response to ICI therapy in

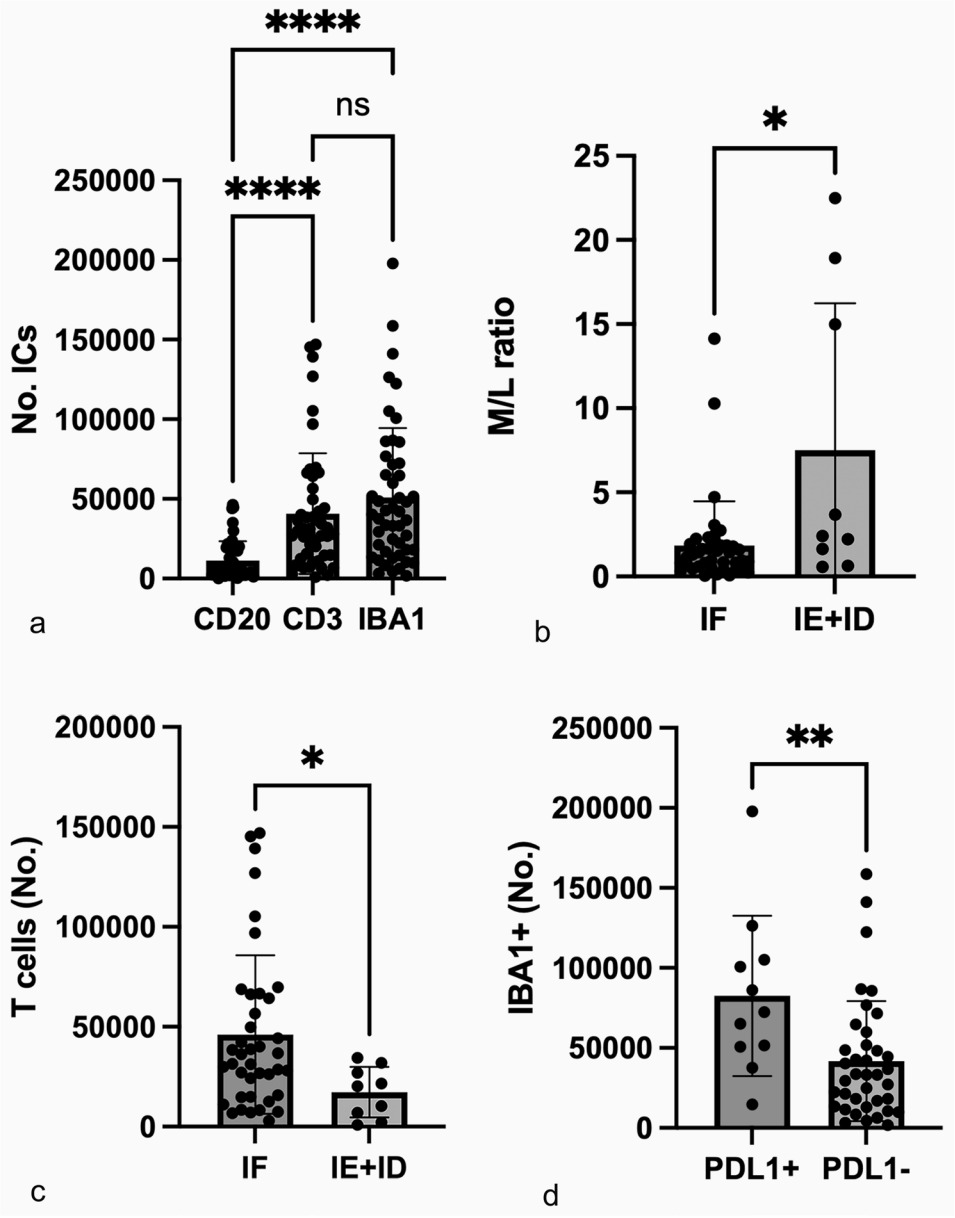

Fig. 2 Results graphs: (**a**) The number of macrophages and T lymphocytes was statistically higher compared to the B cells ($p < 0.0001$ Kruskal Wallis Dunn's multiple comparisons test; **** = asterisks for extremely significant data $p < 0.0001$; ns = non significant) (**b**ratio was significantly lower in immune-inflamed (IF; mean 1.84% SD = 2.62) compared to immune-excluded (IE) and immune-desert phenotypes (ID; mean 7.5% SD = 8.72, $p = 0.02$ Mann-Whitney test; * = asterisk for significant data $p < 0.05$) (**c**) T cells number was significantly higher in the immune-inflamed phenotype (IF) compared to the immune-excluded (IE) and immune-desert (ID) phenotypes ($p = 0.01$ Mann-Whitney test, * = asterisk for significant data $p < 0.05$) (**d**) IBA + cells were more numerous in PD-L1 + tumors than PD-L1- tumors ($p = 0.003$ Mann-Whitney test, ** = asterisks for very significant data $p < 0.001$)

human bladder cancer [31]. However, in order to effectively control tumor progression, T lymphocytes need to infiltrate the tumors first [13]. Hence the importance of evaluating the spatial distribution of T lymphocytes and their use as a pathological parameter for the categorization of predictive classes of ICI response, namely immune-inflamed, -excluded and -desert phenotypes [31].

In the present work, to classify tumors into immunological phenotypes, we qualitatively characterized the spatial distribution of the immune cells of the TIME using multiplex immunohistochemistry. We found that most canine urothelial tumors exhibit an immune-inflamed phenotype (82%), characterized by infiltration of immune cells inside the tumor. Similarly, immune-inflamed are the most common phenotype in human UCs (72%) and the response to atezolizumab (PD-L1

inhibitor), depends on the composition of T cell populations that infiltrate the tumor itself (Powles et al., 2019).

Regarding the composition of the immune microenvironment in the various immune phenotypes, no differences were detected for macrophages, but the immune inflamed phenotype showed a statistically higher number of lymphocytes and a lower macrophage-to-T-lymphocyte ratio, demonstrating its richness in T cells compared to the other immune phenotypes. The detection of the immune-inflamed as the most common phenotype in canine UCs is an interesting finding for therapeutic purposes in dog, since in humans the immune-inflamed phenotype is a promising marker able to predict favorable clinical outcomes of ICI therapy across multiple cancer types [27]. This analogy needs to be confirmed, following the characterization, also in dogs, of the T cell subpopulations that may have opposite roles in tumor immunomodulation [23]. Eto et al. [11] conducted an in-depth analysis of the TIME and its spatial configuration in canine urothelial carcinomas, identifying — as in our case — the presence of an inflamed immune phenotype. Particularly interesting in their study is the observation of a high level of CD3 + and CD8 + T lymphocyte infiltration within the tumor nests in subjects pretreated with COX inhibitors, compared to untreated subjects. In our study, however, clinical comparison could not be performed due to the limited number of cases with available clinical and therapeutic information.

Immune desert tumors are characterized by the absence of T cells in the TIME, and the underlying mechanisms may involve immunological ignorance, induction of tolerance or a lack of appropriate T-cell priming or activation [6].

In the immune-excluded phenotype the accumulated T cells are unable to infiltrate the TIME and this prevention has a stromal-based inhibition derived by multiple chemokines, vascular factors or mediators [6]. TSS available from this caseload are in line with those from literature [5], but the robustness of this data requires a larger cohort of dogs with adequate follow-up.

These results suggest that integrating the diagnosis of UC based on hematoxylin-eosin-stained slides with immunophenotypic assessment may be beneficial in providing additional prognostic information. Regarding the role of ICI in the treatment of canine UCs, the data from the present investigations are not conclusive. No significant differences in TSS were observed between dogs with PD-L1$^+$ UC and those with PD-L1$^-$ tumors; median survival appeared lower in the PD-L1$^+$ group (172 vs. 295 days), but the result was not statistically significant ($p = 0.16$, Log-rank test). However, the relatively small number of PD-L1$^+$ cases likely limited the study's statistical power, increasing the risk of a Type II error and potentially obscuring a true survival difference.

A significant advancement in the knowledge of the TIME in canine UCs has been achieved through multiplex technology, which can analyze multiple markers within the same single tissue section. This technique offers the advantage of colocalizing cells expressing the different markers tested leading to the topographic mapping of the cell populations examined and therefore providing data on spatiality. Computer-aided image analysis is increasingly used in oncology research also in veterinary medicine [25]. Manual scoring for biomarkers quantification is not recommended, because it is subjective and often not reproducible [3]. In addition, machine-learning based digital analysis allows the examination of whole tissue sections, further reducing the subjectivity of the area selection. Objective and reproducible data obtained by whole tissue sections allows to collect high-quality data that can be correlated with clinical parameters for new biomarker selection [3].

In conclusion, most urothelial carcinomas were identified as T cell–rich, immune-inflamed tumors. A subset also expressed PD-L1, which was significantly associated with a high density of IBA1$^+$ cells, suggesting a potential role of tumor-associated macrophages (TAMs) in regulating PD-L1 expression. Further investigation into macrophage polarization in relation to PD-L1 expression is warranted to better elucidate this interaction.

The identification of tumor immune macro-categories, both immunologically reactive and non-reactive, is essential to guide immunotherapy research in pets. We know that this classification is the tip of the iceberg and considering the complexity of TIME [7], a deeper characterization of the diversity of cellular and stromal components is essential to understand and therapeutically redirect niches of reactive immune system in anti-tumor action.

Supplementary Information

The online version contains supplementary material available at https://doi.org/10.1186/s12917-025-05045-8.

Supplementary Material 1. Supplementary Fig. 1. (a) Immunohistochemistry anti-PD-L1, canine urothelial carcinoma: nests of neoplastic cells with positive membranous expression; on the right there are positive immune cells. (b) Multiplex immunohistochemistry anti-CD3 (brown), -CD20 (light blue), -IBA1 (pink), canine urothelial carcinoma: high power field of numerous immune cells in a case of immune-inflamed tumors.

Supplementary Material 2

Acknowledgements
Not applicable.

Authors' contributions
L V.M. and G.S. performed the experimental design and wrote the main manuscript text; G.D.A., F.T., C.T., A.G., M.F., worked on the immunohistochemical methods, B.B. provided support for image analysis, G.A. and D.V. provided part of the carcinoma caseload, P.V. and A.G. provided the clinical follow-up data, All authors reviewed the manuscript.

Funding
This research received no external funding.

Data availability
Raw data and materials are available upon request to the corresponding author.

Declarations

Ethics approval and consent to participate
Histopathology samples were retrieved retrospectively from pathology databases. All previous treatments, including surgery were performed with prior owners' informed consent, as standard of care in veterinary medicine. As part of the informed consent process, the owners also granted permission for the use of archived samples for research purposes.

Consent for publication
Not applicable.

Competing interests
The authors declare no competing interests.

Received: 12 May 2025 / Accepted: 3 September 2025
Published online: 24 November 2025

References

1 Akhtar M, Rashid S, Al-Bozom IA. PD – L1 immunostaining: what pathologists need to know. Diagn Pathol. 2021;16(1):1–11.
2 Bajorin DF, Witjes JA, Gschwend JE, et al. Adjuvant nivolumab versus placebo in Muscle-Invasive. Urothelial Carcinoma. 2021;384(22):2102–14.
3 Bankhead P, Loughrey MB, Fernández JA, et al. QuPath: open source software for digital pathology image analysis. Sci Rep. 2017;7(1):1–7.
4 Binnewies M, Roberts EW, Kersten K, et al. Understanding the tumor immune microenvironment (TIME) for effective therapy. Nat Med. 2018;24:541–50. https://doi.org/10.1038/s41591-018-0014-x.
5 Bradbury ML, Mullin CM, Gillian SD et al. Clinical outcomes of dogs with transitional cell carcinoma receiving medical therapy, with and without partial cystectomy. Can Vet J. 2021;62(2):133–40.
6 Chen DS, Mellman I. Elements of cancer immunity and the cancer–immune set point. Nature. 2017;541:321.
7 Combes AJ, Samad B, Krummel MF. Defining and using immune archetypes to classify and treat cancer. Nat Rev Cancer. 2023;23(7):491–505. https://doi.org/10.1038/s41568-023-00578-2.
8 Davis AA, Patel VG. The role of PD-L1 expression as a predictive biomarker: an analysis of all US food and drug administration (FDA) approvals of immune checkpoint inhibitors. J Immunother Cancer. 2019;7(1):278. https://doi.org/10.1186/s40425-019-0768-9.
9 Deng R, Lu J, Liu X, Peng XH, Wang J, Li XP. PD-L1 expression is highly associated with Tumor-Associated macrophage infiltration in nasopharyngeal carcinoma. Cancer Manag Res. 2020;12:11585–96. PMID: 33209062; PMCID: PMC7669506.
10 Downes MR, Slodkowska E, Katabi N, Jungbluth AA, Xu B. Inter- and intraobserver agreement of programmed death ligand 1 scoring in head and neck squamous cell carcinoma, urothelial carcinoma and breast carcinoma. Histopathology. 2020;76(2):191–200. https://doi.org/10.1111/his.13946.
11 Eto S, Kato D, Saeki K, Iguchi T, Shiyu Q, Kamoto S, et al. Comprehensive analysis of the tumour immune microenvironment in canine urothelial carcinoma reveals immunosuppressive mechanisms induced by the COX-prostanoid cascade. Vet Comp Oncol. 2024;22(4):500–12. https://doi.org/10.1111/vco.12999.
12 Faraj SF, Munari E, Guner G, Taube J, Anders R, Hicks J, Meeker A, Schoenberg M, Bivalacqua T, Drake C, Netto GJ. Assessment of tumoral PD-L1 expression and intratumoral CD8 + T cells in urothelial carcinoma. Urology. 2015;85(3):703e. 1-6. PMID: 25733301; PMCID: PMC4695997.
13 Galli F, Aguilera JV, Palermo B, Markovic SN, Nisticò P, Signore A. Relevance of immune cell and tumor microenvironment imaging in the new era of immunotherapy. J Exp Clin Cancer Res. 2020;39(1):89. https://doi.org/10.1186/s13046-020-01586-y. PMID: 32423420; PMCID: PMC7236372.
14 Galsky MD, Arija JÁA, Bamias A, et al. Atezolizumab with or without chemotherapy in metastatic urothelial cancer (IMvigor130): a multicentre, randomised, placebo-controlled phase 3 trial. Lancet. 2020;395(10236):1547–57.
15 Harada K, Dong X, Estrella JS, Correa AM, Xu Y, Hofstetter WL, et al. Tumor-associated macrophage infiltration is highly associated with PD-L1 expression in gastric adenocarcinoma. Gastric Cancer. 2018;21(1):31–40. https://doi.org/10.1007/s10120-017-0760-3.
16 Lei Q, Wang D, Sun K, Wang L, Zhang Y. Resistance mechanisms of anti-PD1/PDL1 therapy in solid tumors. Front Cell Dev Biol. 2020;8:672. https://doi.org/10.3389/fcell.2020.00672. (PMID: 32793604; PMCID: PMC7385189).
17 Lim SO, Li CW, Xia W, Cha JH, Chan LC, Wu Y, Chang SS, Lin WC, Hsu JM, Hsu YH, Kim T, Chang WC, Hsu JL, Yamaguchi H, Ding Q, Wang Y, Yang Y, Chen CH, Sahin AA, Yu D, Hortobagyi GN, Hung MC. Deubiquitination and stabilization of PD-L1 by CSN5. Cancer Cell. 2016;30(6):925–39. Epub 2016 Nov 17. PMID: 27866850; PMCID: PMC5171205.
18 Maekawa N, Konnai S, Okagawa T, et al. Immunohistochemical analysis of PD-L1 expression in canine malignant cancers and PD-1 expression on lymphocytes in canine oral melanoma. PLoS ONE. 2016;11(6):1–13.
19 Maekawa N, Konnai S, Nishimura M, et al. PD-L1 immunohistochemistry for canine cancers and clinical benefit of anti-PD-L1 antibody in dogs with pulmonary metastatic oral malignant melanoma. NPJ Precis Oncol. 2021;5(1):1–9.
20 Minoli L, Licenziato L, Kocikowski M, et al. Development of monoclonal antibodies targeting canine PD-L1 and PD-1 and their clinical relevance in canine apocrine gland anal sac adenocarcinoma. Cancers (Basel). 2022;14(24):1–12.
21 Muscatello LV, Gobbo F, Avallone G, Innao M, Benazzi C, D'Annunzio G, Romaniello D, Orioles M, Lauriola M, Sarli G. PDL1 immunohistochemistry in canine neoplasms: validation of commercial antibodies, standardization of evaluation, and scoring systems. Vet Pathol. 2024;61(3):393–401.
22 Nguyen SM, Thamm DH, Vail DM, London CA. Response evaluation criteria for solid tumours in dogs (v1.0): a veterinary cooperative oncology group (VCOG) consensus document. Vet Comp Oncol. Sep; 2015;13(3):176–83.
23 Pinard CJ, on behalf of the International Immuno-Oncology Biomarker Working Group, Lagree A, Lu F-I, Klein J, Oblak ML, et al. Comparative evaluation of tumor-infiltrating lymphocytes in companion animals: immuno-oncology as a relevant translational model for cancer therapy. Cancers. 2022;14:5008.
24 Sumitomo R, Hirai T, Fujita M, Murakami H, Otake Y, Huang CL. PD-L1 expression on tumor-infiltrating immune cells is highly associated with M2 TAM and aggressive malignant potential in patients with resected non-small cell lung cancer. Lung Cancer. 2019;136:136–44. Epub 2019 Aug 31. PMID: 31499335.
25 Salvi M, Molinari F, Iussich S, Muscatello LV, Pazzini L, Benali S, Banco B, Abramo F, De Maria R, Aresu L. Histopathological classification of canine cutaneous round cell tumors using deep learning: A Multi-Center study. Front Vet Sci. 2021;8:640944. PMID: 33869320; PMCID: PMC8044886.
26 Sharma P, Shen Y, Wen S, Yamada S, Jungbluth AA, Gnjatic S, et al. CD8 tumor-infiltrating lymphocytes are predictive of survival in muscle-invasive urothelial carcinoma. Proc Natl Acad Sci U S A. 2007;104(10):3967–72. https://doi.org/10.1073/pnas.0611618104.
27 Shen J, Choi YL, Lee T, Kim H, Chae YK, Dulken BW, Bogdan S, Huang M, Fisher GA, Park S, Lee SH, Hwang JE, Chung JH, Kim L, Song H, Pereira S, Shin S, Lim Y, Ahn CH, Kim S, Oum C, Kim S, Park G, Song S, Jung W, Kim S, Bang YJ, Mok TSK, Ali SM, Ock CY. Inflamed immune phenotype predicts favorable clinical outcomes of immune checkpoint inhibitor therapy across multiple cancer types. J Immunother Cancer. 2024;12(2):e008339. https://doi.org/10.1136/jitc-2023-008339. PMID: 38355279; PMCID: PMC10868175.
28 Shosu K, Sakurai M, Inoue K, et al. Programmed cell death ligand 1 expression in canine cancer. Vivo. 2016;30(3):195–204.
29 Singh A, Raja D, Kaushal S, Seth A, Singh P, Sharma A. Phenotypic characterization of tumor associated macrophages and circulating monocytes in patients with urothelial carcinoma of bladder. Immunol Res. 2025;73(1):66.
30 Twomey JD, Zhang B. Cancer immunotherapy update: FDA-approved checkpoint inhibitors and companion diagnostics. AAPS J. 2021;23(2):39. https://doi.org/10.1208/s12248-021-00574-0. (PMID: 33677681; PMCID: PMC7937597).
31 van Dorp J, van der Heijden MS. The bladder cancer immune micro-environment in the context of response to immune checkpoint inhibition. Front Immunol. 2023;14(August):1–13.
32 Verma NK, Wong BHS, Poh ZS, Udayakumar A, Verma R, Goh RKJ, Duggan SP, Shelat VG, Chandy KG, Grigoropoulos NF. Obstacles for T-lymphocytes in the tumour microenvironment: therapeutic challenges, advances and opportunities beyond immune checkpoint. EBioMedicine. 2022;83:104216. https://doi.org/10.1016/j.ebiom.2022.104216. Epub 2022 Aug 17. PMID: 35986950; PMCID: PMC9403334.

33 Wang B, Liu H, Dong X, Wu S, Zeng H, Liu Z, Wan D, Dong W, He W, Chen X, Zheng L, Huang J, Lin T. High CD204 + tumor-infiltrating macrophage density predicts a poor prognosis in patients with urothelial cell carcinoma of the bladder. Oncotarget. 2015;6(24):20204–14.
34 Yagi T, Baba Y, Okadome K, Kiyozumi Y, Hiyoshi Y, Ishimoto T, Iwatsuki M, Miyamoto Y, Yoshida N, Watanabe M, Komohara Y, Baba H. Tumour-associated macrophages are associated with poor prognosis and programmed death ligand 1 expression in oesophageal cancer. Eur J Cancer. 2019;111:38–49. Epub 2019 Feb 26. PMID: 30822683.
35 Zhang H, Liu L, Liu J, Dang P, Hu S, Yuan W, Sun Z, Liu Y, Wang C. Roles of tumor-associated macrophages in anti-PD-1/PD-L1 immunotherapy for solid cancers. Mol Cancer. 2023;22(1):58. https://doi.org/10.1186/s12943-023-01725-x. PMID: 36941614; PMCID: PMC10029244.

Publisher's Note